Repair of Earthquake-Damaged Square R/C Columns with Glass Fiber-Reinforced Polymer

Sassan Eshghi[1], **Vahid Zanjanizadeh**[2]

[1]Assistant Professor of International Institute of Earthquake Engineering and Seismology(IIEES), Email: s.eshghi@iiees.ac.ir

[2]Graduate Student of International Institute of Earthquake Engineering and Seismology(IIEES), Email: v.zanjani@iiees.ac.ir

Abstract: *This paper presents an experimental study on seismic repair of damaged square reinforced concrete columns with poor lap splices, 90-degree hooks and widely spaced transverse bars in plastic hinge regions according to ACI detailing (pre.1971) and (318-02) using GFRP wraps. Three specimens were tested in "as built" condition and retested after they were repaired by glass fiber-reinforced plastic sheets. They were tested under numerous reversed lateral cyclic loading with a constant axial load ratio. FRP composite wraps were used for repairing of concrete columns in critically stressed areas near the column footings. Physical and mechanical properties of composite wraps are described. Seismic performance and ductility of the repaired columns in terms of the hysteretic response are evaluated and compared with those of the original columns. The results indicated that GFRP wraps can be an effective repair measure for poorly confined R/C columns due to short splice length and widely spaced ties with 90-degree anchorage hooks. Both flexural strength and ductility of repaired columns were improved by increasing the existing confinement in critical regions of them.*

Keywords: *Columns, GFRP, Earthquake Damage, Repair, Hysteretic Response, Ductility*

1. Introduction

After major earthquakes, many damaged and undamaged R/C buildings within the affected region need to be repaired and strengthened based on more demanding seismic codes.

Furthermore, many existing reinforced concrete columns were constructed according to older codes, lack adequate seismic resistance. These columns were typically designed for gravity loads and were often inadequately detailed to resist earthquake forces in zones of high seismicity. Most of the columns in older reinforced concrete buildings can be particularly vulnerable structural elements due to inadequate lap splice detailing for the longitudinal bars. They have also lack of confinement in flexural hinge zones and inadequate shear strength.

In addition, field observations in past earthquakes have revealed that columns with inadequate compression lap splices and widely spaced transverse reinforcement performed poorly, especially those located along the perimeter of the buildings. This paper presents the results of an experimental study on a repairing technique for non-ductile concrete columns, having inadequate lap splices for their longitudinal reinforcement, with GFRP sheets applied in plastic hinge regions of them.

2. Background and previous research

Past earthquakes including the San Fernando (California-1971), Loma Prieta (California-1989), Northridge (California-1994), Kobe (Japan-1995), Izmit (Turkey-1999), Chichi (Taiwan-1999), Gujarat (India-2001), Boumerdes (Algeria-2003) and Bam (Iran-2003) caused sever damage and collapse of non-ductile reinforced concrete frames.

Fig.1 Failure of lap splice due to widely spaced ties with 90º hooks (Izmit-1999)

Fig.2 Failure of lap splice due to insufficient splice length and widely spaced ties with 90º hooks (Northridge-1994)

These earthquakes have clearly demonstrated the vulnerability of non-ductile R/C frames and the need for their repair and strengthening.

The most common types of non-ductile details are short splice length and wide ties with 90° hooks. These details had led to considerable damages in recent earthquakes. Fig.1 and Fig.2 show two-column damage in Izmit and Northridge earthquakes due to such detailing.

Since the Loma Prieta 1989 earthquake, considerable progress has been made by many institutions such as the California Department of Transportation in implementing retrofit measures to upgrade the seismic resistance of the columns.

Nowadays, the use of FRP sheets for repairing and strengthening of R/C columns has become widespread. Several researchers have investigated the circular, oval, and rectangular R/C columns and use of fiber reinforced polymer composite jackets for seismic strengthening and repair of columns with deficiencies such as inadequate lap splice for the longitudinal reinforcement or lack of the sufficient shear strength [Chai et al., 1991[4], Marsh, 1992[5], Xiao et al., 1999[11], Xiao et al.,1997[12], Bayrak et al., 1997[2], Bayrak et al., 2003[3], and Wallace et al., 2004[10]].

Chai, et al. investigated the use of fiber composite wraps for retrofit of the circular concrete columns and Bayrak et al. and Xiao et al. studied retrofit of rectangular columns with CFRP. Marsh examined the use of steel angle and straps and steel jacketing to strengthen of rectangular R/C columns with inadequate lap splices.

Past researches have been extensively directed toward repair and retrofit of damaged bridge columns, for instance in [9] typical damaged bridge R/C columns have been tested. But, a few researches have been carried out on the behavior and/or using of FRP sheets for retrofitting of rectangular R/C columns of buildings with deficient lap splices and/or inadequate confinement under various axial and lateral cyclic loading [3] [10]. The reported research in this paper, addresses the repair of damaged square R/C

Table 1 Detail of test specimens

Specimen	$P/f'_c A_g$	Axial load (kN)	Layers of GFRP	ρ_{sh} %	Splice 20 d_b
SP-S1	0.05	21.2	0	0.644	No
SP-S_2	0.05	21.2	0	0.258	Yes
SP-S_3	0.15	63.6	0	0.258	Yes
SP-R_1	0.05	21.2	5	0.644	No
SP-R_2	0.05	21.2	5	0.258	Yes
SP-R_3	0.15	63.6	5	0.258	Yes

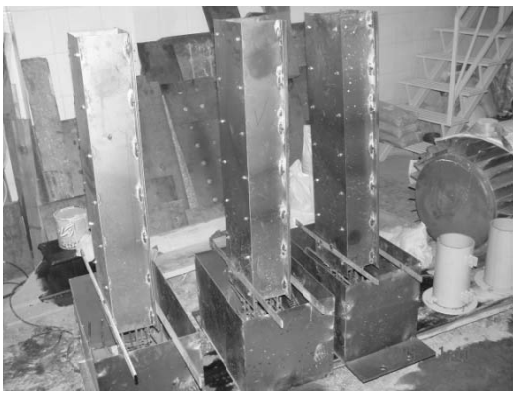

Fig.3 Specimens reinforcing cage in their formworks

Fig.4 Strain gauges were installed on the bars

columns of buildings with defective detailing via glass fiber-reinforced wraps.

3. Experimental work

Three R/C columns were severely damaged as part of research. The columns were cast in an upright position using normal weight aggregate concrete, and cured for periods exceeding 28 days. This experimental program consisted of the design, construction, testing of three columns under cyclic loading, and subsequently repaired prior to retesting with same loading. The main variable item was the level of axial load in all the specimens.

The specimens were cantilever columns with the fixed end framing into rectangular spread footings. Two of the specimens had longitudinal bars with short splice lengths, widely spaced transverse reinforcement, cut off more than 50% of the moment capacity of the section according to ACI (pre.1971). One of them was in accordance with ACI (318-02) detailing.

3.1. Specimens

All columns had square cross sections of 150×150-mm, 1000-mm length, reinforced by 8-mm diameter longitudinal bars. Two of them have 4-mm ties @150-mm spacing with 90º hooks according to ACI (pre.1971) detailing and one of them has 4-mm ties@60-mm in plastic hinge region and @150-mm in other sections with 135°hooks

Table 2 Properties of reinforcing steels [13]

Bar size	f_y (MPa)	ε_y	E_s (MPa)	f_u (MPa)	ε_u
8M	420	0.00168	2.3719×10^5	640	0.115
4M	300	0.00146	2.051×10^5	500	0.129

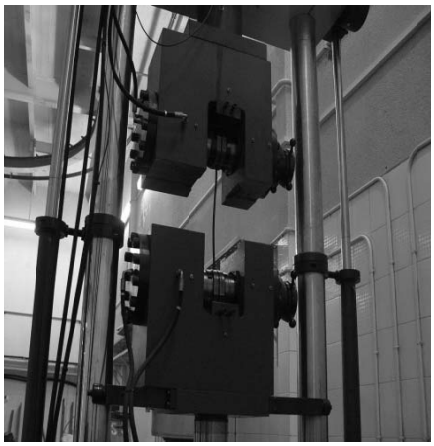

Fig.5 Longitudinal bar under tension test

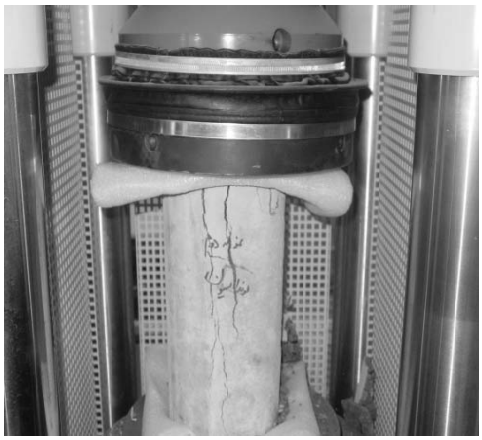

Fig.6 Cylindrical sample under compression test

in accordance with ACI(318-02) detailing.

The lateral load is applied at 800-mm from the base of column. The specimens represent columns located in multistory building frame between of the maximum moment and contra flexure points. Details of the specimens are listed in Table 1.

3.2. Material properties

A series of basic tests was carried out to obtain the mechanical properties of concrete and reinforcing steel. Reinforcing bars and GFRP sheet and concrete were tested to obtain mechanical characteristic of materials. Grade 400, steel were used for longitudinal and grade 300 steel for transverse steel bars. Fig. 5 shows a bar under tension test. Critical stress and strain of reinforcing steel obtained from the tension tests, are listed in Table 2.

The concrete mix had water cement ratio of 0.5. Portland cement, Type 2, was used in this study. The average slump was 120.2-mm. Three 152.5×305-mm (6×12 in) cylindrical samples were tested to obtain the concrete compressive strength (Fig. 6).

Maximum size of the aggregates was 15-mm. All the columns and foundations were cast vertically and were vibrated with a vibrator rod. The average nominal concrete strength at 28 days (f'_c) was 18.9 MPa.

Columns were confined by being wrapping in a continuous manner with bidirectional GFRP sheets and corrosion resistant, vinyl ester resin matrix. Glass fiber has been used for different civil engineering applications. Because of an economical balance of cost and specific strength, glass fiber-reinforced polymer used in this study. E-glass comprises approximately 80 to 90 percent of glass fiber commercial production used in this study.

Table 3 Mechanical properties of FRP composite

Coefficient of thermal expansion 10^{-6}/C	Tensile modulus (MPa)	Tensile strength (MPa)	Density (N/mm^3)	Strain to failure (percent)
4.7	70000	1750	25.5	4.8

Table 4 Mechanical properties of vinyl ester resin

Heat distortion Temperature (C)	Tensile modulus (MPa)	Tensile strength (MPa)	Tensil elongation at break(percent)
119	3171	89.6	5.2

The mechanical properties of GFRP composite and vinyl ester resin are summarized in Table 3 and 4.

3.3. Reinforcing details

Three specimens have been constructed and tested. The structural configuration of the specimens consisted of two parts, a stub cage and a column cage. They were built separately and then connected to each other. Fig. 7 shows the detailing of specimens reinforcement. Column type C1detailing was designed according to ACI (pre.1971). Column type C2 was designed according to ACI (318-02). Detailing of both types of footings designed to be strong enough to prevent cracking.

3.4. FRP Installation

All three specimens in as-built condition were tested and then were repaired by first replacing the loosened concrete with quickset cement then were cleaned with a high pressure gun and completely dried before the vinyl ester was applied to their surfaces (Fig.8). Special measures were taken to ensure that there were no voids between the sheets and the concrete surfaces. After the application of the first layer of the GFRP sheet, a second layer of vinyl ester sheet was applied on the surface of the first layer to allow impregnation of the second layer of the GFRP sheet.

The wrapping of the columns continued to the upper region of the column (Fig.9). All the repaired specimens were cured at least for 7 days to ensure that full strength had obtained before testing.

3.5.Test setup

Fig.10 illustrated the loading assembly used to apply the gravity and lateral loads. An actuator with 50 kN capacity was used to impose predefined cyclic displacement routine at top end of the columns. The axial load was applied with a 250 kN capacity hydraulic jack. This testing setup was able to consider the P-Δ effect that might be experienced in buildings. The bottom of the specimens were connected and fixed to the strong floor.

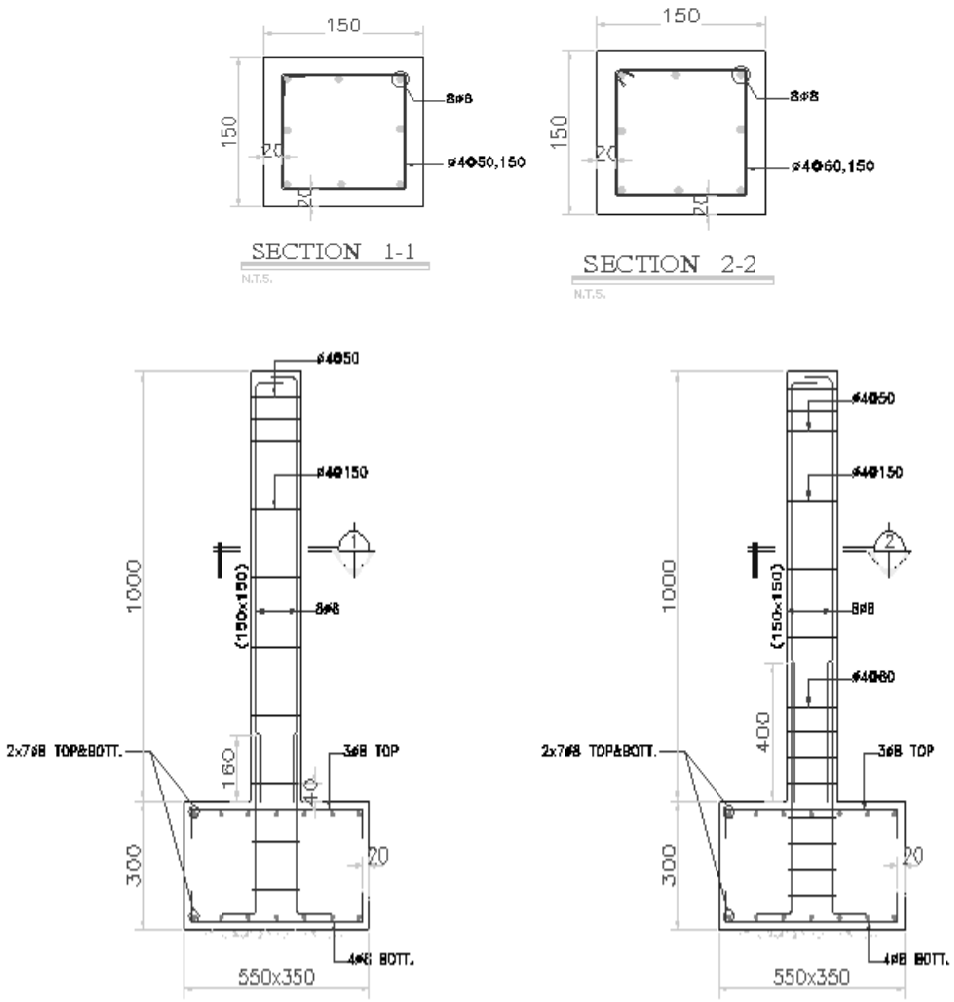

Fig. 7 Specimens geometry and details (a) Column Type C1 (b) Column Type C2

Fig.8 Cleanig surface of the damaged columns

Fig.9 Installation of prefabricated composit sheets

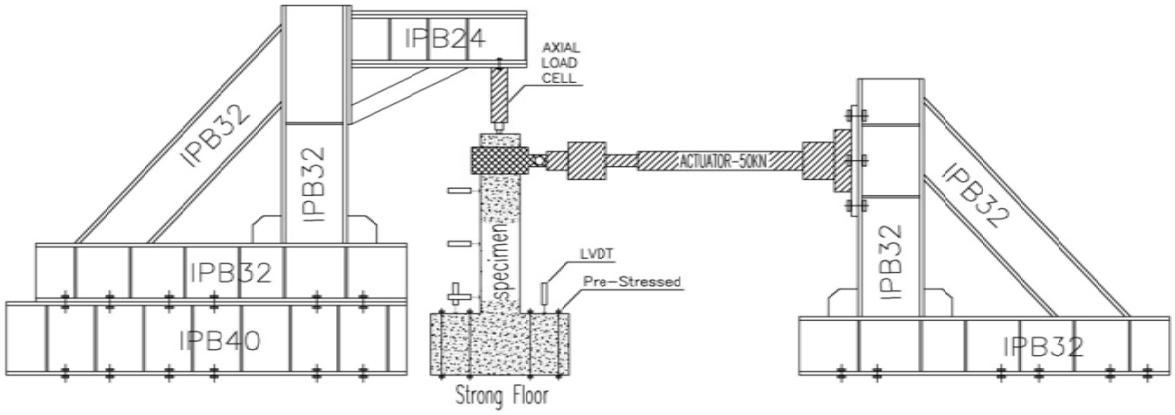

Fig.10 Schematic test setup

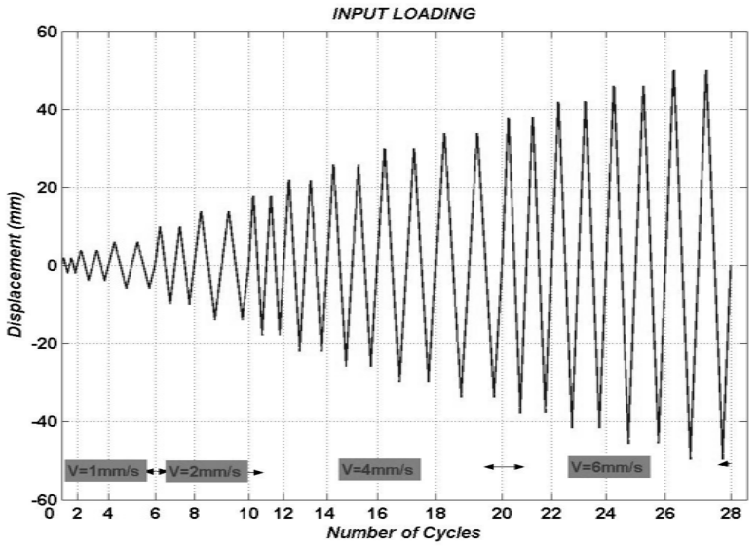

Fig.11 Lateral displacement history

The height of the columns was 1000-mm but lateral displacement was applied at a height of 800-mm of the columns.

3.6. Testing procedure and instrumentation

Predefined cyclic lateral displacements with 28 cycles were subjected to specimens while the axial load was constant at either (0.05f'c Ag) or (0.15f'c Ag). Each prescribed drift level repeated twice in order to measure the strength degradation of the specimens.The rate of the applied displacement is shown in Fig. 11.

Each specimen was instrumented to record various response parameters. Linear Variable Differential Transformers (LVDT s) were installed on the specimens to measure the rotations of the columns relative to footings and also probable vertical displacements of the supports and the footings due to the lateral forces. All specimens were instrumented with three strain gauges on rebars (see Fig.4), two strain gauges on the surface of FRP sheets and two strain gauges on the surface of the columns, just above the FRP sheets.

a) Specimen SP-S1 b) Specimen SP-S2 c) Specimen SP-S3

d) Specimen SP-R1 e) Specimen SP-R2 f) Specimen SP-R3

Fig.12 Specimens at end of testing

4. Test results

Behavior of a specimen under loading, was graphically represented in the form of a relationship between the hysteretic moment and the curvature of the section. Stiffness degradation and distribution of cracks were studied in the as built and also the repaired columns. In each cycle the lateral load and the deflection at free end of the columns were recorded and the crack patterns were registered during the tests.

4.1. Observed damages and behavior

During testing of specimen SP-S1 at 1% drift ratio, initial flexural cracks were observed at the column footing interface and at 1.5% drift ratio the same cracks at the column footing splice length. Some flexural cracks appeared along the splice length during the test but the length and width of these cracks did not increase significantly (Fig.12a).

In specimen SP-S2 flexural cracks on the column face started as early as at 1% lateral drift ratio. At this time longitudinal cracks were formed at right and left sides of the specimen. During the second cycle at 3.5% drift as fairly large sections of the concrete cover spalled at the column footing interface. The lateral load strength diminished, indicating that bond along the spliced bars was deteriorating. Shear cracking was observed at 2.5% drift but these cracks were not significant throughout the test. Damage in this specimen was severer than that in the

previous one (Fig.12b).

Specimen Sp-S3 was subjected to a (0.15 A_g f'_c) constant axial load and initial flexural longitudinal cracks suddenly appeared at 1.5% drift ratio. In this test, cracking formed later but cracking propagation developed suddenly as the load applied. In this specimen the cover spalled completely at the corner at 4.5% drift ratio and the longitudinal bars were clearly visible. Along the splice length, there was severe damage. Shear cracks were observed at 3.5% drift ratio on the right and left faces of the columns and concrete crushing and spalling were observed just before the end of the test. In this specimen damage was generally severer than SP-S1 and SP-S2 (Fig.12c).

Stiffness of the repaired specimens had been deteriorated under large reversed cyclic loading. Large amount of the damages were concentrated in FRP sheets and some small sheet rupture was observed in high drift ratio. Damage in the concrete of repaired columns was slight. Vertical and horizontal flexural cracking, that occurred above the FRP jacket in past testing, opened and closed during retesting. Nevertheless, in the SP-R1, damage was very low and very little stress concentration was occurred in FRP sheets. Some new cracks were observed in all repaired specimens but they were not significant. At the end of the test, cracks in all specimens propagated along the columns but in SP-R3 the sustained damage was more serious than two others. Cracks in SP-R1 were little and narrow. During the test, cracks at the column footing interface of SP-R3 were very serious and some spalling and crushing were appeared. So it indicated that high axial load led to more serious damage in the specimens. SP-R1 behaved better and no delaminating or rupture across the fibers of the jackets was observed in this specimen (Fig.12d, 12e, 12f).

4.2. Moment- curvature response

The total moment at the bottom of the columns is calculated by summing up the moments caused by the lateral load and the vertical load due to lateral displacement as given by Equation (1), follow as

$$M=F.\ h +P\Delta_{Lateral}. \quad (1)$$

The curvature values were obtained from deformation reading at middle of the column and bottom LVDTs data located at 100-mm above the column footing interface.

4.3. Ductility and energy dissipation parameters

To quantify the response of columns under imposed loads, it is preferred to define the response indices that can describe their behavior quantitatively. In most current seismic design methodologies, the inelastic deformation is generally quantified by ductility parameters. Since the member ductility can not be applied for this series of displacement control tests, only section ductility is described. Moment-curvature diagram and its corresponding ductility parameters can be utilized to describe the ductility of the specimens.

Fig.14 describes some ductility parameters including curvature ductility factor μ_ϕ, cumulative ductility ratio N_ϕ and energy damage indicator E. Subscripts t and 80 are added, respectively, to N_ϕ, E to indicate the value of each parameter at two different occasions: end of the test and end of the cycle in which the moment is dropped to approximately 80 percent of the maximum value. In Fig14, L_f represents the length of the most damaged region measured during the test and h represents the depth of the column section.

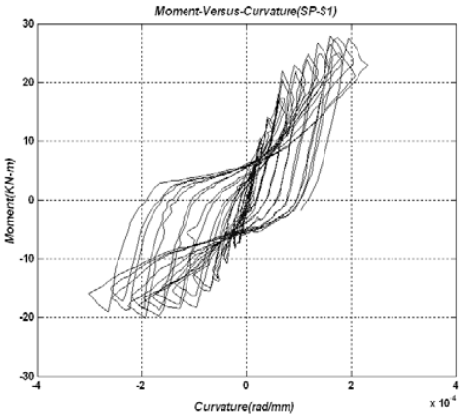

a)SP-S1

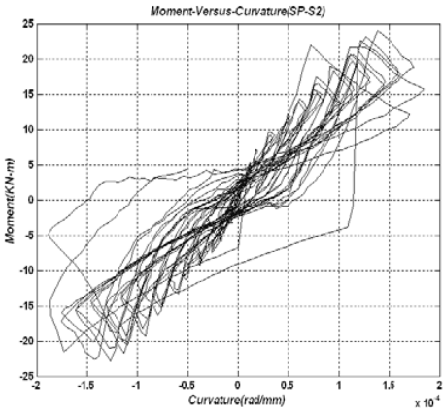

b)SP-S2

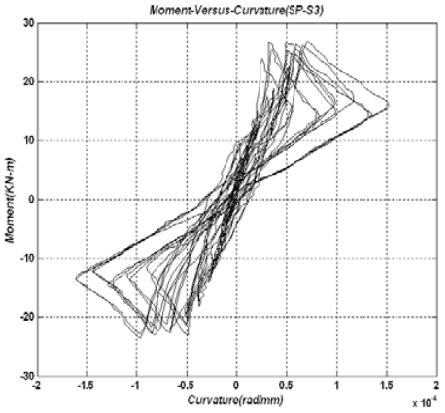

c) SP-S3

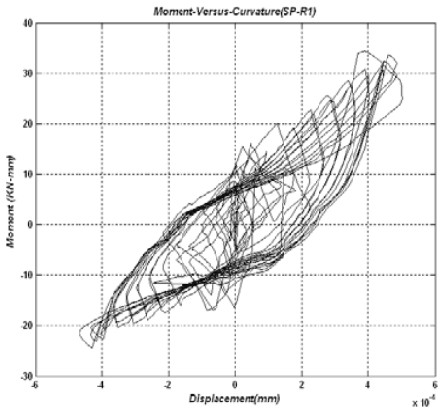

d) SP-R1

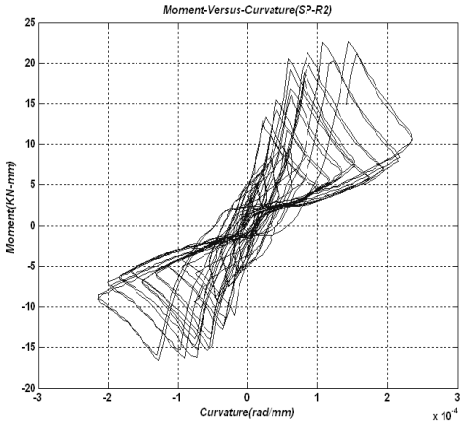

e) SP-R2

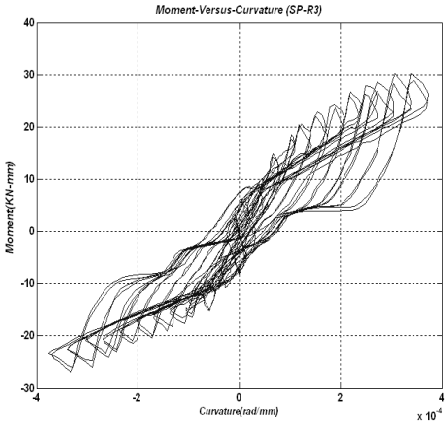

f) SP-R3

Fig.13 Moment –Curvature diagrams of the specimens

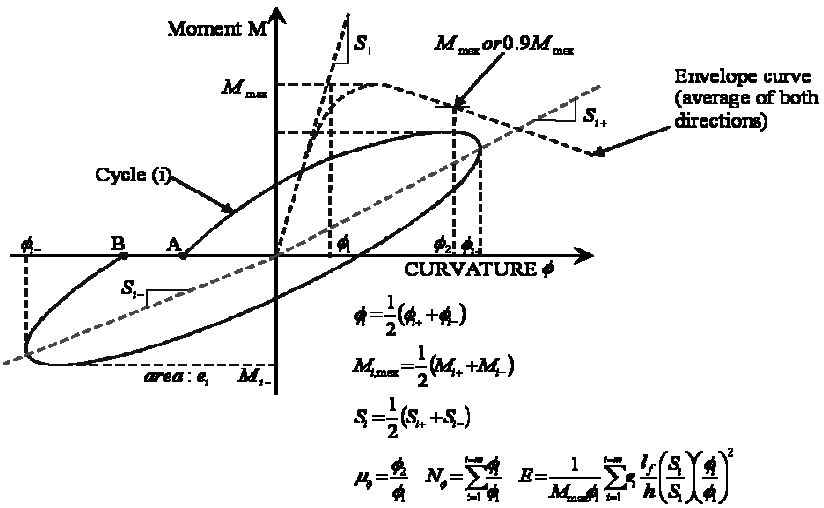

Fig.14 Definitions of section ductility parameters

Table 5 Section ductility parameters

Specimen	$\mu_{\phi 80}$	$N_{\phi 80}$	$N_{\phi t}$	E_{80}	E_t
SP-S1	+	+	44.6	+	1180.2
SP-S2	4	29.05	38.4	580.7	786.3
SP-S3	3.09	24.13	45.8	165.2	423.9
SP-R1	+	+	55.5	1059.8	1333.2
SP-R2	+	+	59.9	673.5	891.9
SP-R3	+	+	51.1	352.6	537.2

+=moment did not drop to this level

The curvature ductility parameters and energy damage indicator for all the specimens are listed in Table 5.

4.4. Stiffness degradation

Stiffness for each cycle was calculated as the average of the stiffness for the positive and negative directions. Stiffness for each cycle was normalized with respect to the stiffness of the first cycle and was plotted versus the displacement. Stiffness degradation versus column top displacement after normalization is plotted in Fig.15 and Fig.16.

4.5.Effect of GFRP repairing technique on damaged columns

For assessing a repair technique, a single parameter criterion can not be adequate in many cases. Herein, various parameters are employed to evaluate the applied repairing method. SP-S2 and SP-R2 have the same detailing and were subjected to the same axial loading but SP-R2 was repaired with GFRP wraps after testing. Experiments indicated that total cumulative ductility ratio ($N_{\phi t}$), 80% of energy indicator (E_{80}) and total energy indicator (E_t) were increased by 25%,

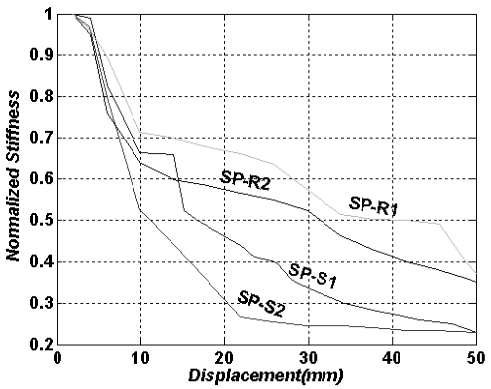

Fig.15 Normalized Stiffness versus Displacement for SP-S1, SP-S2, SP-R1and SP-R2

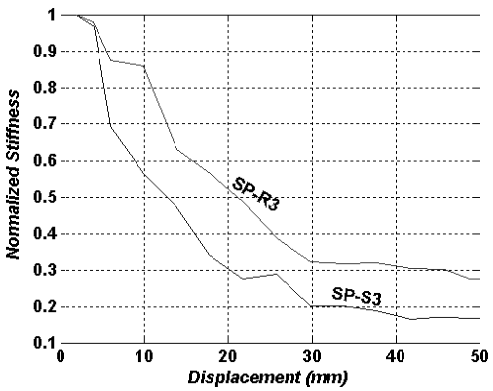

Fig.16 Normalized Stiffness versus Displacement for SP-S3, SP-R3

16% and 14% for SP-R2. These percentages for SP-S3 and SP-R3 were 12%, 113% and 27%.The results of total cumulative ductility and damage indicator for SP-S1, with the same loading condition, were 16% and 50% which were greater than those for SP-S2.

4.6.Axial load effect

SP-S1, SP-S2, SP-R1 and SP-R2 were under a defined axial load. SP-S3 and SP-R3 were under a different axial load. Increasing axial loads of the specimens led to reductions in ductility parameters. Curvature ductility factor ($\mu_{\phi 80}$) in SP-S2 was 30% higher than that in SP-S3. Moreover, the cumulative curvature ductility ratio showed reduction from 29.05 to 24.13 for $N_{\phi 80}$ and from 45.8 to 38.4 for $N_{\phi t}$ in original specimens and from 45.8 to 51.1 for $N_{\phi t}$ as a result of repairing the damaged specimens. Similar conclusions can be drawn on energy damage indicators, E_{80} and E_t. A higher axial load led to decrease in the energy dissipation and increase in the rate of stiffness degradation and adversely affected the cyclic performance of the repaired and as-built specimens.

5. Summary and conclusions

R/C columns with insufficient longitudinal splice length accompanied by widely spaced transverse ties and 90° hooks poorly in recent earthquakes and in some instances may have played a significant role in the partial or total collapse of some buildings. Three square R/C columns were constructed with reinforcement details typical of ACI (pre.1971) and (318-02). The columns were initially damaged under axial and lateral loading to high damage state. The damaged columns were subsequently repaired with GFRP and tested again. The following conclusions are drawn from the test results of the seismically deficient columns before and after repairing.

- Observing of the columns damage revealed that compression lap splice with widely spaced transverse reinforcement performed poorly.

- Ductility, flexural strength and energy dissipating of SP-S1 were significantly higher than SP-S2 and SP-S3. This Indicated

that sufficient lap splice length and also confining of concrete in plastic hinge region in the R/C. columns improved their seismic performance significantly.

- Use of the GFRP sheets for repairing of damaged columns changed the flexural plastic hinge location from the base of the columns to a place just above the GFRP sheets.

- GFRP composite wraps were effective in restoring the flexural strength, stiffness and ductility capacity of damaged columns and enhancing the shear strength and concrete confinement in the damaged columns.

- In all repaired specimens, the rate of stiffness deterioration under constant axial load and reversed cyclic loading was lower than original columns. However, the initial stiffness of repaired columns were lower than of the original columns.

- In all specimens, the rate of degradation was dependent on the level of the axial loading and also to the level of the applied shear force. At high level of axial load differences in ductility, energy dissipating and stiffness degradation between the as-built and repaired columns were considerable.

- Repaired specimens behavior demonstrated stable loops in high drift ratios and performed as a better energy dissipater compared to the original specimens.

- The repaired columns showed relatively larger lateral displacements at low load levels compared to the original columns. This appeared to be due to pre-existed damage in the form of bond deterioration between reinforcing bars and concrete in original columns and cracks induced during the first test. However, the lateral strength of the repaired columns increased compared to the original columns.

6. Acknowledgements

The authors wish to thank International Institute of Earthquake Engineering and Seismology (IIEES) for sponsoring and supporting the research reported in this paper. They would also like to acknowledge Ms. Maedeh Alemi for her technical assistance.

7. References

[1] Aboutaha , R.S., Engelhardt ,M.D., Jirsa, J.O., Kreger, M.E., (1996), Retrofit of Concrete Columns with Inadequate Lap Splices by the Use of Rectangular Steel Jackets, Earthquake Spectra, November ,Vol.12, PP. 693-715.

[2] Bayrak , O., Sheikh, S. A., (1997), High-Strength Concrete Columns under Simulated Earthquake Loading, ACI Structural Journal, Vol. 94, No. 6, November- December, PP.708-722.

[3] Bayrak, O., Lacobucci, R.D., Sheikh , S. A., (2003), Retrofit of Square Concrete with Carbon Fiber-Reinforced Polymer for Seismic Resistance , ACI Structural Journal ,Vol .100 , No. 6, November-December ,PP.785-794.

[4] Chai, Y. H., Priestley, M.J.N., Seible, F., (1991), Seismic Retrofit of Circular Bridge Columns for Enhanced Flexural Performance, ACI Structural Journal, Vol.88, No. 5, September- October, PP.572-584.

[5] Marsh, L.,(1992) "Seismic Retrofits for R/C Columns Bar Splices,"

Proceedings of the 1992 Structures Congress, ASCE, San Antonio, Texas, April 13-15, 1992.

[6] Paulay, T., Priestley, M.J.N. (1992), Seismic Design of Reinforced Concrete and Masonry Building, John Willey & Sons INC, New York.

[7] Penelis, G., Kappos, A. J., (1997), Earthquake - Resistant Concrete Structures, E &FN Spon Published.

[8] Priestley, M.J.N., Seible, F., Xiao, Y., Verma, R., (1994), Steel Jacket Retrofitting Concrete Bridge Columns for Enhanced Shear Strength-Part 2: Test Results and Comparison with Theory, ACI Structural Journal, Vol .91, No. 5, September – October, PP.537-551.

[9] Saadatmanesh, H., Ehsani, M.R., Jin L., (1997), Repair of Earthquake-Damaged RC Columns with FRP Wraps, ACI Structural Journal, Vol.94, No. 2, March-April, PP.206-215.

[10] Wallace, J. W., Melek, M., (2004), Cyclic Behavior of Columns with Short Lap Splices, ACI Structural Journal, Vol .101, No. 6, November – December, PP. 802-811.

[11] Xiao , Y., Wu ,H., Martin ,G.R., (1999), Prefabricated Composite Jacketing of RC Columns for Enhanced Shear Strength , Journal of Structural Engineering, ASCE, Vol.125 , No.3, March, PP.255-264.

[12] Xiao, Y., Ma, R., (1997), Seismic Retrofit of RC Circular Columns Using Prefabricated Composite Jacketing, Journal of Structural Engineering, ASCE, Vol. 123, No.10-12, PP.1357-1364.

[13] Zanjanizadeh, V. (2005), Experimental and Analytical Approach to Repair and Retrofit of the Reinforced Concrete Columns for Earthquake Resistance, M.Sc. Thesis, Supervised by Sassan Eshghi, International Institute of Earthquake Engineering and Seismology, IRAN (in Persian).

8. Notations

The following symbols are used in this paper:

A_g=gross area of column, mm^2
E= energy-damage indicator
E_s= modulus of elasticity of steel, MPa
f'_c=compressive strength of concrete determined from 150x300 mm cylinders, MPa
f_u=ultimate strength of steel, MPa
f_y = yield strength of reinforcing steel bars, MPa
L_f=length of most damaged column region, mm
N_ϕ=cumulative curvature ductility ratio
P=axial load applied to column section, kN
ε_u=strain at ultimate stress in steel
ε_y=yield strain in steel
μ_ϕ=curvature ductility factor
ρ_{sh}=volumetric ratio of transverse ties to concrete core
ϕ=curvature of most damaged column region, rad/mm
ϕ_1=curvature obtained from M-ϕ curve corresponding to maximum moment on straight line joining origin and a point at 65% of M_{max}, rad/mm
ϕ_2=curvature obtained from M-ϕ curve corresponding to 80% of M_{max} on descending portion of curve, rad/mm.